"As members of the Clemson University community, we have inherited Thomas Green Clemson's vision of this institution as a 'high seminary of learning'. Fundamental to this vision is a mutual commitment to truthfulness, honor, and responsibility, without which we cannot earn the trust and respect of others. Furthermore, we recognize that academic dishonesty detracts from the value of a Clemson degree. Therefore, we shall not tolerate lying, cheating, or stealing in any form."
"I certify that all the writing that I contributed to here is my own and not acquired from external sources. I have cited sources appropriately and paraphrased correctly. I have not shared my writing with other students, nor have I acquired any written portion of this document from past or present students."
Signed by: Jason Lagoa, Dylan Holtzhauer, Christopher Young

# Modeling and Analysis of Pendulum Cart System

Dylan Holtzhauer[1], Jason Lagoa[2], and Christopher Young[3]

*Clemson University, Clemson, SC, 29631*

**The motivation for this experiment was to model the motion of a complex dynamic system, that system being a cart-pendulum apparatus. The ability to model these dynamic systems is beneficial in the sense that the behavior of the system can be predicted, typically accurately. Once the simulation of the model is confirmed as an accurate representation of the system, parameters can easily be changed, and the responses are quick to simulate. To model this dynamic system, several system parameters had to be identified for the cart-pendulum. With those parameters, the equations of motion were found as non-linear differential equations, which were then linearized using Taylor series expansion. Using these equations of motion, the dynamic system can be simulated using Simulink, both for the nonlinear equations of motion and the linear equations of motion. The mass of the cart and the damping coefficient for the cart and pendulum were also calculated using the log decrement method since these parameters were unable to be easily measured. The experimental results, nonlinear simulation, and linearized simulation were then compared to each other. The results show that the spring constant was found to be 118 N/m. Using these values in the simulations yielded extremely similar initial responses, however, they undershoot on the rebound, which implies**

[1] Student, Mechanical Engineering.
[2] Student, Mechanical Engineering.
[3] Student, Mechanical Engineering.

**the spring constant is off. They also do not settle as fast, which implies the damping coefficients are low.**

## Nomenclature

| | | |
|---|---|---|
| $m_1$ | = | mass of cart (kg) |
| $m_2$ | = | mass of pendulum (kg) |
| $x$ | = | linear displacement (m) |
| $\Theta$ | = | angular displacement (radians) |
| $c$ | = | linear damping coefficient (kg/s) |
| $b$ | = | angular damping coefficient (kg/s) |
| $k$ | = | spring constant (N/m) |
| $F_P$ | = | reaction force of pendulum (N) |
| $R$ | = | length of pendulum rod (m) |
| $T$ | = | torque (N*m) |
| $I$ | = | moment of inertia (kg*m$^2$) |
| $g$ | = | acceleration due to gravity (m/s$^2$) |
| $\omega_n$ | = | natural frequency (radians/second) |
| $\omega_d$ | = | damping frequency (radians/second) |
| $\zeta$ | = | damping ratio (N/A) |
| $\delta$ | = | logarithmic decrement (N/A) |
| $P$ | = | period (seconds) |
| $u_w$ | = | uncertainty function |
| $W$ | = | generic function |
| $f_1$,$f_2$ | = | generic functions |
| $f$ | = | generic function |

## I.Background

BEING able to model dynamic systems is a useful tool in engineering. Modeling a dynamic system allows engineers to essentially predict the behavior of a system, typically using ordinary differential equations. These ordinary

differential equations can also be simulated using some software. For this lab specifically, a cart pendulum system was analyzed using an optical encoder and a load cell sensor. An optical encoder is essentially a motion sensor that is meant to detect rotational (or linear) motion using a light source and photosensitive detectors, and this motion is converted into an electrical signal [1]. The optical encoder was used to detect the rotation of the pendulum in this system, and the electrical signal that the rotational motion output was recorded using a data acquisition (DAQ) system. A load cell is similar to an optical encoder in that it converts something mechanical into an electrical signal, but a load cell does this for an applied force [2]. In this case, when the cart was in motion an electrical signal was recorded by the DAQ due to the load cell, and the translational motion of the cart could be analyzed.

## II.Experimental Method

To set up the mass pendulum system for analysis later, care had to be taken in what data was collected and how the experiment was set up. Prior to collecting data with a DAQ, some data points were manually collected. The mass and length of the pendulum could be directly recorded. The k value of the spring was experimentally calculated by applying a known force and measuring displacement. Then the transducer for the cart was calibrated by moving the cart a certain distance and recording the voltage from the transducer.

From there, the recording of experiments began. The cart was held still while the pendulum was swung, then the pendulum was removed, and the cart was released from a position. This helped determine the values of the mass of the cart and the damping for the cart and pendulum. The system was then recoupled and released from rest.

Extra experiments were conducted, which included adding mass to the pendulum, tilting the entire frame, and bounding the movement of the cart. The data for both the mass position and pendulum angle were recorded and exported into a text file to be analyzed at a later time.

Following the data collection, the equations of motion of the system were determined by analyzing the free-body diagrams of the cart and pendulum individually, and they were then linearized using Taylor expansion. With the non-linear and linear equations of motion known, the motion of the cart pendulum system was then modeled using Simulink.

## III.Analysis of Experimental Data

### A. System Schematic and Non-Linear Equations of Motion

Below the schematic of the cart-pendulum system is shown, along with the free-body diagrams for the cart and pendulum individually.

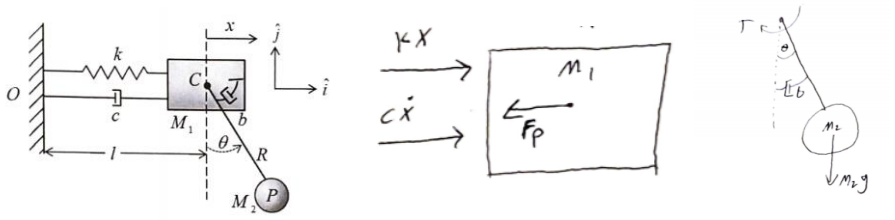


a) b) c)

**Fig. 1 System Schematic (a) and Accompanying Free-Body Diagrams of Cart (b) and Pendulum (c)**

Analyzing Fig. 1b, the equation of motion for the uncoupled cart can easily be obtained. There is only translational movement in the horizontal direction, so only the sum of forces acting in the horizontal direction will be considered. This equation is shown below.

$$\Sigma F_{X,cart} = m_1\ddot{x} = F_p - kx - c\dot{x} \tag{1}$$

To determine $F_p$, the translational equation of motion for the pendulum needs to be determined. This is accomplished by analyzing the free-body diagram of the uncoupled pendulum shown in Fig. 1c, however, this equation of motion is not as simple as the one for the uncoupled cart. Due to this, a more in-depth derivation for this equation of motion is shown below.

$$\Sigma F_{x,pend} = m_2 \frac{d^2}{dt^2}[x - R\sin(\Theta)] = F_p \tag{2}$$

$$\Sigma F_{x,pend} = m_2[\ddot{x} - R\ddot{\Theta}\cos(\Theta) + R\dot{\Theta}^2\sin(\Theta)] = F_p \tag{3}$$

In equation 2, as opposed to just having an $x$ there is the term $x + R\sin(\Theta)$, and this is due to the fact that when evaluating the acceleration on a free-body diagram, that acceleration is evaluated at the center of mass of that object. Therefore, to account for the acceleration of the pendulum at its center of mass the term $R\sin(\Theta)$ must be added to the typical $x$ term.

To relate these translational equations of motion, equation 3 can be substituted into equation 1, because they have a shared term $F_p$, and the translational equation of motion for the system is shown below.

$$\Sigma F_{x,system} = (m_1 + m_2)\ddot{x} = -m_2R\ddot{\Theta}\cos(\Theta) + m_2R\dot{\Theta}^2\sin(\Theta) - kx - c\dot{x} \tag{4}$$

$$\ddot{x} = \left(\frac{1}{m_1 + m_2}\right)[-m_2R\ddot{\Theta}\cos(\Theta) + m_2R\dot{\Theta}^2\sin(\Theta) - kx - c\dot{x}] \tag{5}$$

For equation 5, a simple division was performed to isolate the $\ddot{x}$ term.

Analyzing Fig. 1c again, it is shown that the pendulum also has a rotational component. Therefore, the rotational equation of motion for the pendulum must be derived. The derivation for this equation of motion is shown below and is explained following these equations.

$$\Sigma M = I\ddot{\Theta} = -T - m_2 gRsin(\Theta) - b\dot{\Theta} \tag{6}$$

$$T = (m_2\ddot{x})Rcos(\Theta) \tag{7}$$

$$I = m_2R^2 \tag{8}$$

$$m_2R^2\ddot{\Theta} = -(m_2\ddot{x})Rcos(\Theta) - m_2gRsin(\Theta) - b\dot{\Theta} \tag{9}$$

$$m_2R\ddot{\Theta} = -(m_2\ddot{x})cos(\Theta) - m_2gsin(\Theta) - \frac{b\dot{\Theta}}{R} \tag{10}$$

$$\ddot{\Theta} = \left(\frac{1}{m_2R}\right)[-(m_2\ddot{x})cos(\Theta) - m_2gsin(\Theta) - \frac{b\dot{\Theta}}{R}] \tag{11}$$

Equation 6 was determined from a simple analysis of the moments acting on the pendulum, which is again shown on the free-body diagram in Fig. 1c. As shown in the equation, the forces acting on the pendulum causing it to rotate are a torque, a component of the pendulum's weight, and the damping caused by the friction at the pin where the pendulum is attached to the cart. Equation 7 is a simple definition of torque, which is a force times the perpendicular distance, and this now gives the variable for torque in terms of parameters that are known. Equation 8 is the definition for the moment of inertia about a fixed point, and it is assumed that the pendulum is rotating about a fixed point (the pin), which again provides that term in terms of known and useful parameters. These redefined variables are then substituted into equation 6, and that is shown in equation 9. Finally, for simplification purposes, the whole equation is divided by the term R, which is the distance of the pendulum's arm, and doing so produces equation 10 which is the equation of motion for the rotation of the pendulum. Equation 10 was determined by performing another simple division similar to that in equation 5 to isolate the $\ddot{\Theta}$ term.

### B. Linear Equations of Motion

The equations of motion for this system are not linear, as shown by having trigonometric functions and certain squared terms in equations 5 and 11. It is not feasible to analytically solve a non-linear ordinary differential equation, to they will be linearized using Taylor expansion. The general equation for Taylor expansion is shown below.

$$f(x,\Theta) = f(x_0,\Theta_0) + \frac{\partial f}{\partial x}|_{x=x_0,\Theta=\Theta_0}(x-x_0) + \frac{\partial f}{\partial \Theta}|_{x=x_0,\Theta=\Theta_0}(\Theta-\Theta_0) \tag{12}$$

In equation 12, the values $x_0$ and $\Theta_0$ are arbitrary and typically small values. For this application, $x_0$ and $\Theta_0$ will both be evaluated as 0. Applying equation 12 to equations 5 and 11 will provide the following linear equations of motion. The full derivations for these can be found in Appendix A.

$$\ddot{x} = \left(\frac{1}{m_1+m_2}\right)[-m_2R\ddot{\Theta}\cos(\Theta) - kx - c\dot{x}] \tag{13}$$

$$\ddot{\Theta} = \left(\frac{1}{m_2R}\right)[-(m_2\ddot{x}) - m_2g(\Theta) - \frac{b\dot{\Theta}}{R}] \tag{14}$$

### C. **Parameters**

The motion of the cart-pendulum system explained by equations 5 and 11 is dictated by a set of parameters that describe force and energy-loss components inherent to every dynamic system. Several parameters were determined prior to experimentation including the mass of the pendulum ($m_2$) and the length $R$ using a weight scale and tape measure respectively. Through the use of a spring scale to measure force and a ruler the spring constant k was determined through the linear correlation between force and distance described in equation 15.

$$F = kx \tag{15}$$

The remaining parameters required experimental data in order to determine based on a log decrement method. Log decrement method describes a data analysis technique in which the peaks of a decreasing sinusoidal graph are compared to determine the damping ratio and damped frequency of a simple oscillatory system. By removing the pendulum from the slider the system then becomes analogous to the oscillating system as a function of damping ratio and damped frequency seen in equation 16.

$$\ddot{x} + \left(\frac{1}{m_1}\right)[cx + kx] \equiv \ddot{x} + \dot{2}\zeta\omega_n\dot{x} + {\omega_n}^2x \tag{16}$$

$$\delta = \frac{1}{n}\ln\frac{x(t)}{x(t+nP)} \tag{17}$$

$$\zeta = \frac{\delta}{\sqrt{4\pi^2+\delta^2}} \tag{18}$$

$$P = \frac{2\pi}{\omega_d} \tag{19}$$

$$\omega_d = \omega_n\sqrt{1-\zeta^2} \tag{20}$$

$$\omega_n = \sqrt{\frac{k}{m_1}} \tag{21}$$

$$\zeta = \frac{c}{2\sqrt{km_1}} \tag{22}$$

The log decrement method seen in equation 17 is the natural log relationship between the amplitude values of consecutive peaks in the oscillating system. Using the delta value found in equation 17 the damping ratio can be solved for in equation 18. Solving for the damped frequency using the oscillating period in equation 19, the natural frequency can then be solved for in equation 20. Lastly, with both the damping ratio and natural frequency calculation, the mass of the slider and the damping coefficient *c* can be solved for in equations 21 and 22. This same method is replicated with the slider held stationary and allowing the pendulum to swing freely in order to determine the damping coefficient *b* in equation 11.

Below is an example of the log decrement method visualized with the estimated damping curve created using the calculated damping ratio and natural frequency. The graph illustrates the analytical precision that the log decrement method utilizes to estimate system parameters for damped oscillating motion.

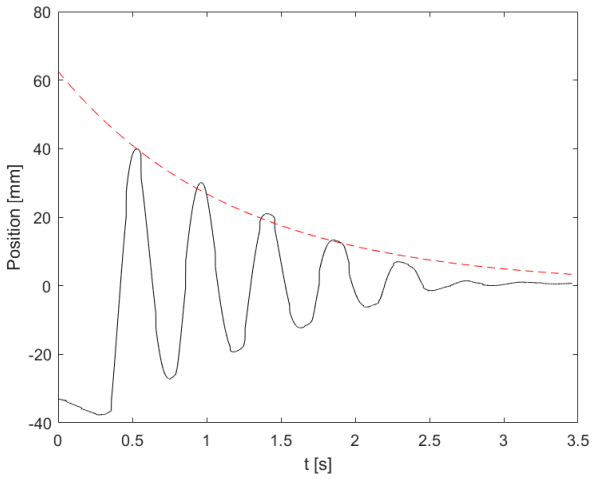


**Fig. 2 Visualization of Log Decrement Method**

## IV. Experimental Results

### A. System parameters

As mentioned in the previous experimental methods section, multiple measuring tools and analytical methods were used to determine all system parameters describing the dynamic motion of the cart and slider.

**Table 1 System Parameters**

| System Parameter | Calculated Value | Units |
|---|---|---|
| Mass of Slider ($m_1$) | 1.04 | $kg$ |
| Mass of Pendulum ($m_2$) | 1.45 | $kg$ |
| Spring constant ($K$) | 118 | $\frac{N}{m}$ |
| Rod Length ($R$) | 0.368 | $m$ |
| Angular damping coefficient ($b$) | 0.022 | $\frac{kg}{s}$ |
| Linear damping coefficient ($c$) | 1.50 | $\frac{kg}{s}$ |
| Damping Ratio for Cart ($\zeta$) | 0.0585 | [-] |
| Natural Frequency for Cart ($\omega_n$) | 12.29 | $\frac{rad}{s}$ |
| Damping Ratio for Pendulum($\zeta$) | 0.0015 | [-] |
| Natural Frequency for Pendulum ($\omega_n$) | 5.25 | $\frac{rad}{s}$ |

### B. Decoupled System

To find system parameters such as the mass of the cart, and damping for the cart and pendulum, the system was decoupled. The results are shown below.

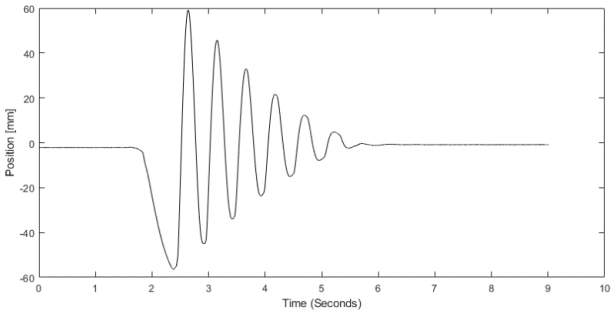


**Fig. 3 Cart Position of Decoupled System**

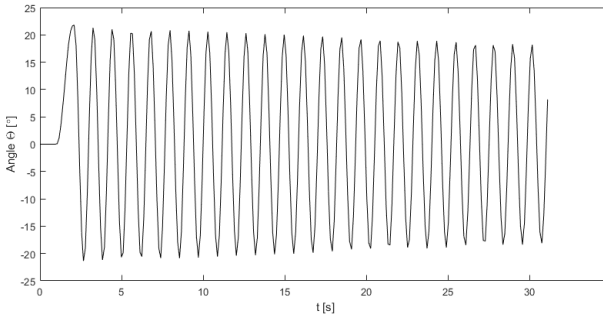


**Fig. 4 Pendulum Angle of Decoupled System**

## C. Coupled System

For the coupled system, the cart was moved back 68mm from rest and released. Data was recorded until the system came to rest.

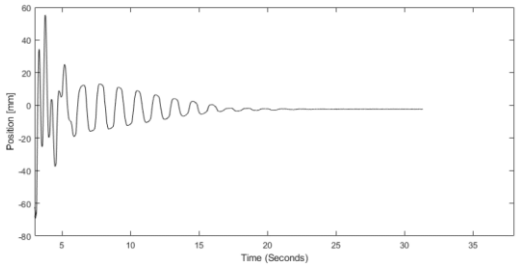


**Fig. 5 Experimental Cart Position of Coupled System**

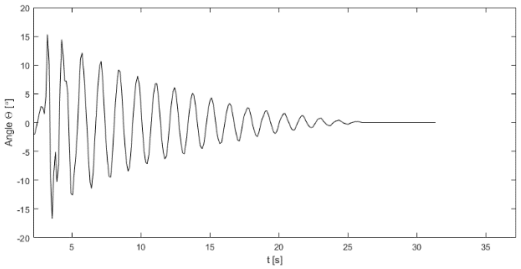


**Fig. 6 Experimental Pendulum Angle of Coupled System**

## D. Tilted System

For the tilted system, the frame was tilted ~45°, then the cart was moved to its original rest position then released. The data for the pendulum angle was lost, so that will not be shown.

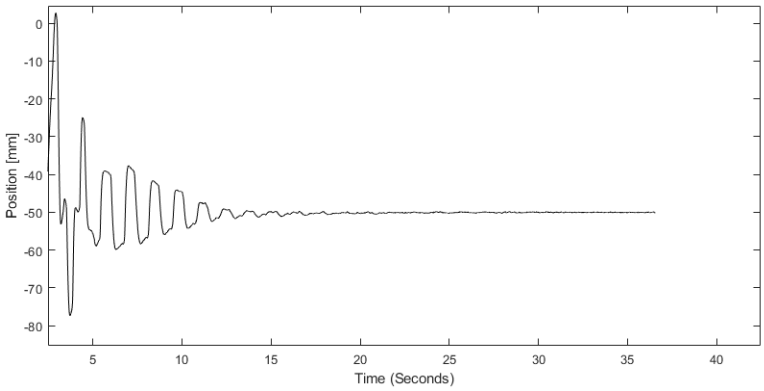


**Fig. 7 Experimental Cart Position of Tilted System**

## E. Added Mass System

For this experiment, a mass was weighed and added to the pendulum. The specific amount of mass added to the end of the pendulum was 958 grams.

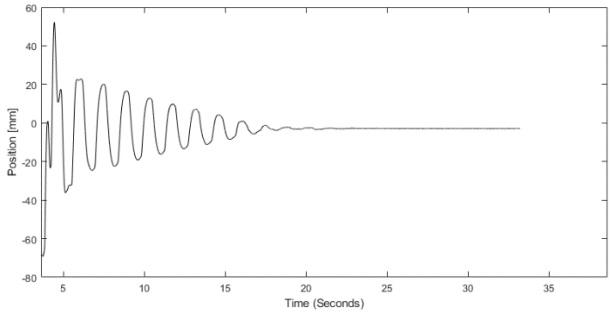


**Fig. 8 experimental Cart Position of Added Mass System**

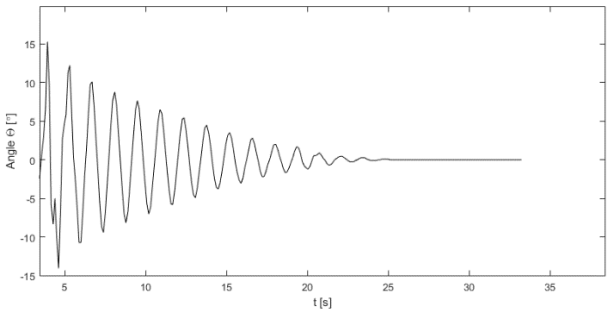


**Fig. 9 Experimental Pendulum Angle of Added Mass System**

## F. Restricted Cart System

For this experiment, the cart's movement was restricted with stops on the linear rails. The cart was pulled back 18mm and released, then recorded until rest.

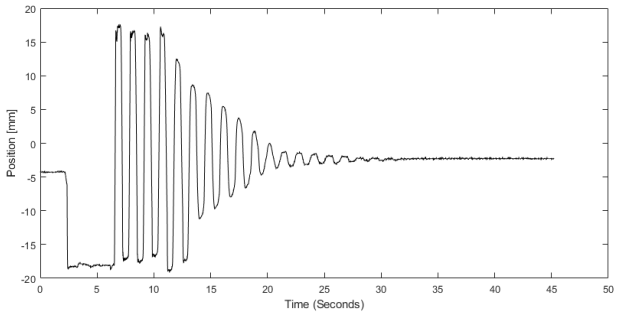


**Fig. 10 Experimental Cart Position of Restricted Cart System**

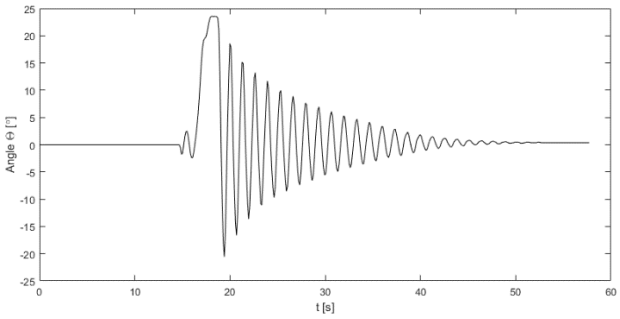


**Fig. 11 Experimental Pendulum Angle of Restricted Cart System**

\

## V. Simulink Models

### A. Non-linear Simulink Model

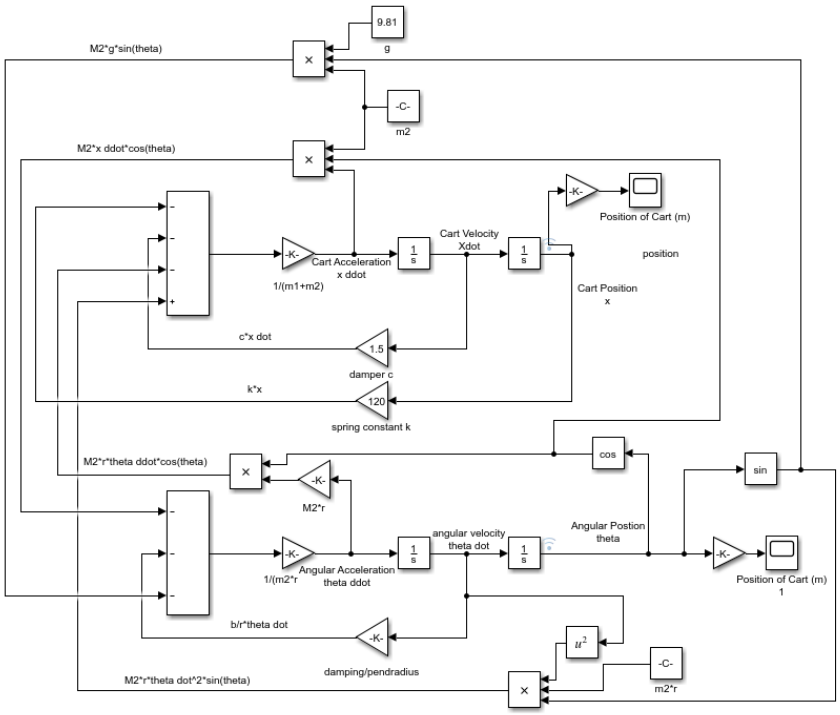

**Fig. 12 Non-linear Simulink Model**

### B. Linearized Simulink Model

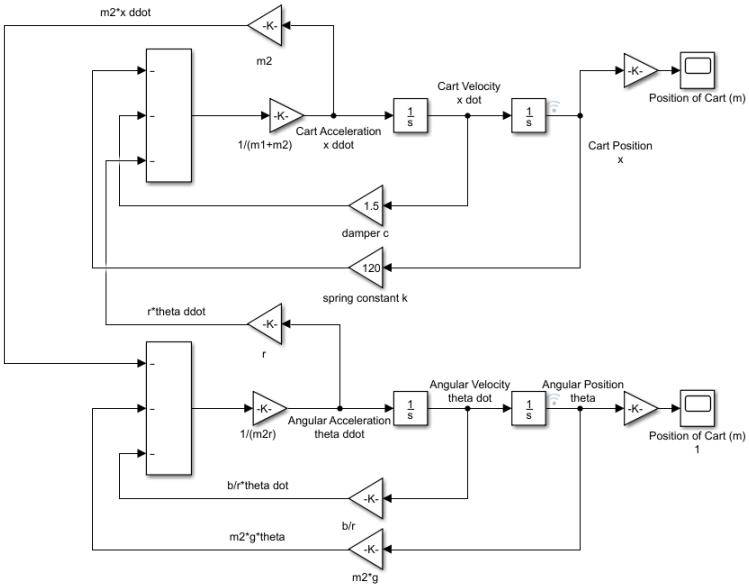


**Fig. 13 Linearized Simulink Model**

## VI. Modeling Results

The systems were modeled in Simulink with the equations of motion, then the parameters were set and the simulations were run. This was first done with the non-linear simulation as non-linear terms were part of the equations of motion. The equations of motion were linearized with Taylor Series Expansion, then modeled and simulated in Simulink as well.

### A. Coupled System

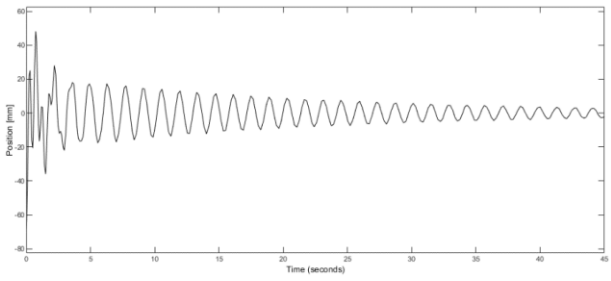


**Fig. 14 Non-linear Simulated Cart Position of Coupled System**

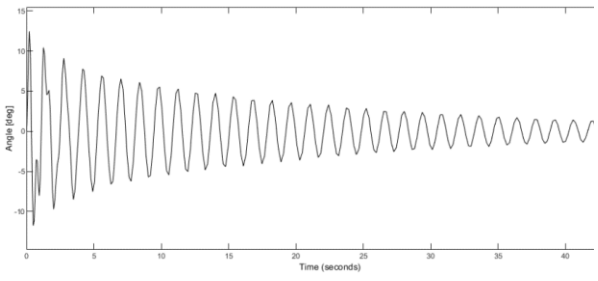


**Fig. 15 Non-Linear Simulated Pendulum Angle of Coupled System**

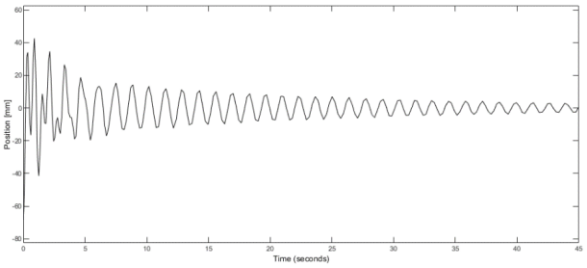


**Fig. 16 Linearized Simulated Cart Position of Coupled System**

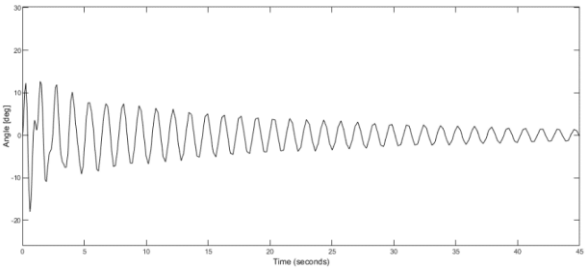


**Fig. 17 Linearized Simulated Pendulum Angle of Coupled System**

B. **Tilted Model**

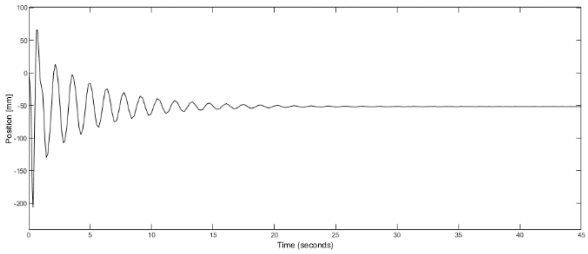


**Fig. 18 Non-linear Simulated Cart Position of Tilted System**

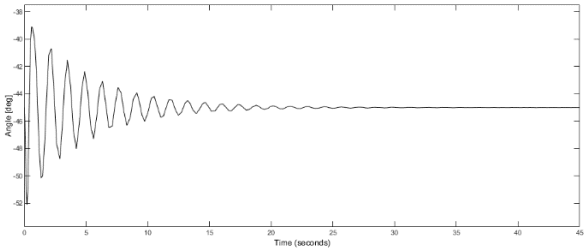


**Fig. 19 Non-Linear Simulated Pendulum Angle of Tilted System**

C. **Added Mass Model**

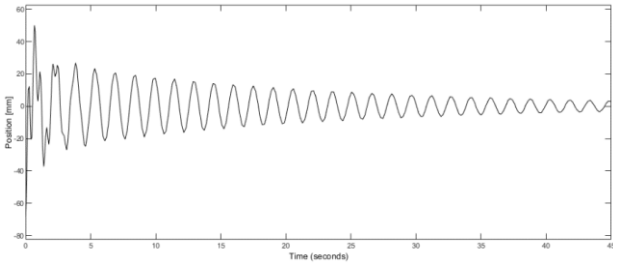


**Fig. 20 Non-linear Simulated Cart Position of Added Mass Model**

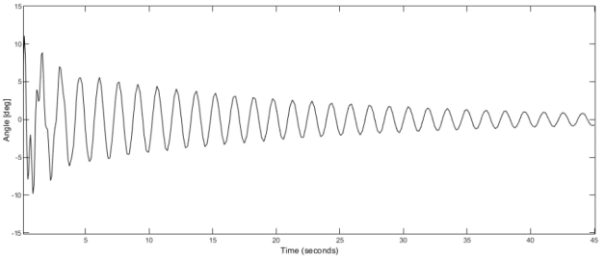


**Fig. 21 Non-linear Simulated Pendulum Angle of Added Mass System**

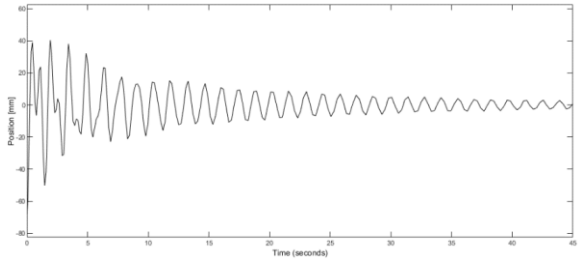


**Fig. 22 Linearized Simulated Cart Position of Added Mass System**

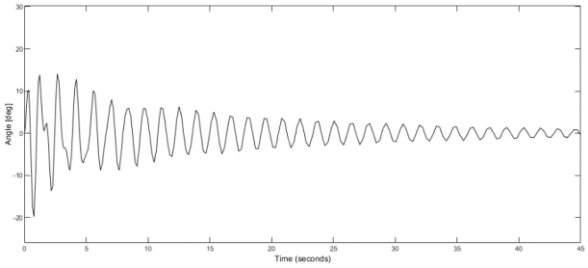


**Fig. 23 Linearized Simulated Pendulum Angle of Added Mass System**

## VII.Discussion

### D. Comparison of Coupled System Results

*1. Cart Position*

For the coupled system, after being released from 68mm, it experimentally rebounds to 55mm, as shown in Fig. 5. For the non-linear system, it rebounds to 50mm, and the linearized system rebounds to 40mm in Fig. 14 and 16 respectively. This could be from miscalculations of the mass of the cart or spring constant, but by this point, the damping should not have had an effect. The initial response for the experimental, non-linear, and linearized versions are extremely similar. A comparison can be seen below in Fig. 24.

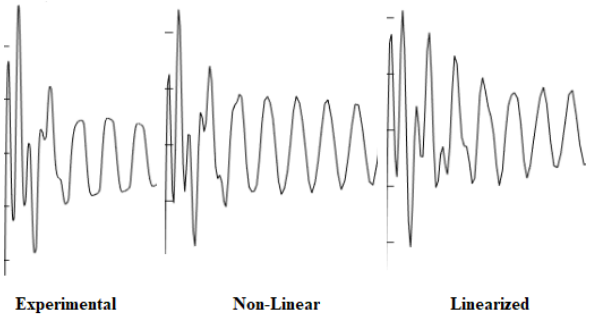


**Fig. 24 Coupled Results Comparison**

Figure 24 above shows roughly the first 10 seconds of the response. The first 5 seconds show an uncanny resemblance with the change in peaks for the experimental and non-linear results being almost indistinguishable. The linearized version is similar, though it is farther off than the non-linear version.

The frequency for all three versions is ~0.8 Hz, which is good, however, the simulations begin to be less accurate farther along. Comparing the full response in Fig. 5, 14, and 16 for the position of the cart for the coupled system, it can be seen the experimental version has much more damping than either the non-linear or linearized version. This implies the value for the damping coefficient for the cart is not what it should be. The experimental version settles in ~18 seconds, while the non-linear and linearized versions settle in ~40 seconds.

*2. Pendulum Angle*

The pendulum angle for the experimental version peaks at ~15 degrees, while the non-linear version peaks at ~12.5 degrees, and the linearized version peaks at ~10 degrees, as shown in Fig. 6, 15, and 17, respectively. This could be due to the inaccuracy of the value used for the radius, as it may not have been at the true center of gravity, or the mass of the pendulum was not recorded properly. The spring constant could have also affected the angular position, as that feeds back into the angular acceleration by accelerating the cart.

The pendulum's time to settle remains higher for the simulations, similar to the cart's settling time. This could be due to an inaccurate value used for the pendulum damping, though it's more likely the inaccurate value for the carts damping feeding back into the pendulum.

## E. **Comparison of Tilted System Results**

*1. Cart Position*

The simulation was not remodeled as a linearized simulation; however, the equations of motion were remodeled for the non-linear simulation. The frequency for both the experimental and non-linear model is ~0.8 Hz,

the same as the standard coupled version, as shown in Fig. 7 and 18, which matches in both the experiment and simulation. The cart's first position peak for the simulation is far more drastic than the experimental version, ~70mm rather than 0mm. The initial response's waveform doesn't match as closely as with the standard coupled system in this case either. However, it does settle to the same value of -50mm for both the experiment and non-linear simulation. It is hard to say why this is. Given the waveforms don't match as well, it may have been a modeling error.

*2. Pendulum Angle*

The experimental pendulum data for the tilted system was lost, so there's no comparison to make. However, when analyzing Fig. 19, the final value it settles to match the angle the frame is tilted, which is what is expected.

## F. Comparison of Added Mass System Results

*1. Cart Position*

The frequency for all three versions is ~0.8 Hz, as shown in the experimental, non-linear, and linearized responses in Fig. 8, 20, and 22 respectively. This frequency is the same as the standard coupled version and tilted version. However, the initial response is less chaotic than the standard coupled version, which makes sense with added mass making it harder to accelerate, therefore being less susceptible to sudden changes in direction. The cart's first position peaks for the different versions match the characteristics of the standard coupled system, with the experimental being ~57mm, the non-linear being ~52mm, and the linearized one being ~40mm. The simulations also take much longer to settle, implying the damping coefficient from the cart is still too low.

*2. Pendulum Angle*

Most of what was said for the pendulum angle in the standard coupled version can be said here as well. The peak values for the pendulum angle in the non-linear simulation were still lower than the experimental values, as shown in the experimental, non-linear, and linearized responses in Fig. 8, 20, and 22 respectively. The peak rebound values being ~15 degrees for the experimental, ~12.5 for the non-linear simulation. However, the linearized simulation peaks to ~-20 degrees. This is likely due to inaccuracies generated by the linearized model.

## G. Discussion of Restricted Cart System

*1. Cart Position*

The position of the cart in the restricted system is heavily altered, resembling a square wave graph for the first several cycles rather than a sinusoidal graph. An important observation is that the frequency during the restricted motion portion resembles that of the unbounded system, however, when the system no longer moves to the distance limiting stoppers it settles to a lower frequency of about 0.7 Hz. This indicates that a significant portion of the energy is removed in losses during the collisions with the bump stops such that the oscillatory portion of the dynamic motion that no longer hits the stops is not identical to the free motion at a similar range of motion. This is a critical observation to make because in a situation where modeling was required to represent a system with distance constraints it would not be accurate to assume free motion and apply a square wave at the point of distance limitation.

*2. Pendulum Angle*

The pendulum in the restricted motion system did not exhibit the same directional changes as the free motion system. Where the original model would have varying peaks and change its direction frequently, the restricted motion moved in an almost linear trend from one peak to the next extremely quickly. Similar to how the cart was not representative of the original coupled system, the pendulum motion is not represented accurately under the assumption that a restricted distance would not alter the dynamic pattern.

## H. **Uncertainty**

Uncertainty is present in all the experimental calculations due to the resolution of all measuring devices as well as potential inevitable system noise. In this experiment, the load cell roughly has an uncertainty of about 0.02% [2]. Other sources of uncertainty that are difficult to quantify can be found in friction along the rods and in the pendulum joint as well as assumptions in the system that are not represented in the real world, for example, the assumption of a massless spring is impossible and difficult to quantify in the dynamic equations. Determining the uncertainty of each measuring device and compounding uncertainty propagation allowed for the calculation of uncertainty for all parameters displayed in table 2 below. Note that the largest error is noted in the spring constant, partially due to the relative size of the parameter compared to the other values, but more notably due to the inaccurate measuring devices used to estimate the value. On the contrary, the angular damping coefficient has the smallest relative uncertainty due to the accuracy of the mass of the pendulum calculation found using a mass scale. These differences highlight the importance of utilizing high accuracy measuring devices to prevent uncertainty propagation from significantly altering

the confidence of experimental data. Uncertainty propagation was determined using the method of partial differentiation according to equation 23 below, and the consecutive equations describe the exact uncertainty equations used for each of the calculated parameters [4].

$$u_w = \pm \sqrt{\sum_{i=1}^{n} (\frac{\partial W}{\partial x_i} u_i)^2} \tag{23}$$

$$u_k = \sqrt{(\frac{1}{x} u_F)^2 + (\frac{F}{x^2} u_x)^2} \tag{24}$$

$$u_{m_1} = \frac{1}{\omega_n^2} u_k \tag{25}$$

$$u_c = \frac{\zeta}{\sqrt{k m_1}} \sqrt{(k u_{m_1})^2 + (m_1 u_k)^2} \tag{26}$$

$$u_b = 2\zeta \omega_n u_{m_2} \tag{27}$$

**Table 2 System Parameters Uncertainty's**

| System Parameter | Uncertainty (±) | Units |
|---|---|---|
| Mass of Slider ($m_1$) | 0.0132 | kg |
| Mass of Pendulum ($m_2$) | 0.0005 | kg |
| Spring constant ($K$) | 2 | $\frac{N}{m}$ |
| Rod Length ($R$) | 0.05 | in |
| Linear damping coefficient (c) | 0.0135 | kg/s |
| Angular damping coefficient (b) | $7.7\ X\ 10^{-6}$ | kg/s |

## VIII. Conclusions and Recommendations

### A. System Parameters

Utilization of the log decrement method allowed for experimental data to dictate the majority of system parameters required to accurately model the system. This method introduced a higher probability of error and is likely responsible

for a significant amount of deviation from the modeled systems. For example, when calculating the delta value in the log decrement method, three separate uncoupled slider motion readings were utilized, each of which provided varying results that increased proportion to the increase in initial distance. This indicates that there are likely other non-linear energy losses in the system that are not accounted for in the system of equations we generated. Other manual calculations, in specific the spring constant were likely sources of deviation due to the method of calculation. Fig. 2 highlights the presence of error sources in the system by visualizing the exponentially decreasing envelope generated from the log decrement method. Several peaks of the experimental data are not restrained in the envelope, indicating that the system is not fully described by the equations of motion proposed by the theoretical calculations.

### B. Non-linear System

The non-linear system did a good job of representing the system as the waveform's initial response in all experiments was almost indistinguishable from the experimental data. The frequency was also fairly close. However, the peak response and long-term response were a bit off. The peak response would likely be due to inaccurate values used for the mass of the components and the spring constant, as the dampers wouldn't have much effect during a short duration. This is compounded by the fact the settling time for the cart and pendulum were longer, meaning that damping constants needed to be higher, which would lower the peak values even more. The accurate initial response leads to the conclusion that the system was modeled correctly, however, the peaks and settling time being incorrect likely means the parameters were inaccurate, or that something else isn't being considered.

### C. Linearized System

Most of what was said in the non-linear section remains true for the linearized version, with the main conclusion being that the difference in peaks and settling time was likely due to inaccurate parameter values. However, the linearized system was even farther off from the experimental data than the non-linear data. This leads to the conclusion that the linearized model is a compromise. This means that while the values are likely simpler to calculate as you can remove non-linear terms, you trade that off for some accuracy, at least in this case.

### D. Recommendations

Some recommendations to improve the methods and results of this lab would be to try and find a better position for the ruler used to measure the distance the cart was traveling. It was difficult to ensure the cart was being moved the desired distance, both while calibrating the cart as well as when taking the actual data of the cart's movement. This

could have provided some inaccurate parameter values since the data provided from the motion of the cart was used when calculating some parameters with the logarithmic-decrement method. Another potential recommendation would be to take the effective mass of the spring into account. During this analysis, the spring was essentially treated as massless, which is obviously not true. If the effective mass of the spring was determined, that could be taken into account (assuming it was not negligibly small), and a more accurate system simulation could be conducted, as well as receiving more accurate parameters. Furthermore, the spring gauge was difficult to hold still while compressing the spring to determine its spring constant. To improve this, the spring gauge could be hooked or attached to the frame so the force needed to compress the spring and displacement of the spring could easily be recorded, allowing for a more accurate spring constant value.

## Appendix

**A.**

The following equations show the derivation for the linearized equations of motion, starting with the translational equation of motion. The general equation used to linearize these can be found in equation 12.

$$f_1(x,\Theta) = \ddot{x} = \left(\frac{1}{m_1+m_2}\right)[-m_2R\ddot{\Theta}\cos(\Theta) + m_2R\dot{\Theta}^2\sin(\Theta) - kx - c\dot{x}] \quad \text{A1}$$

$$\ddot{x} = \left(\frac{1}{m_1+m_2}\right)[-m_2R\frac{d^2}{d\Theta^2}\Theta\cos(\Theta) + m_2R\frac{d}{d\Theta}\Theta^2\sin(\Theta) - kx - c\frac{d}{dx}\dot{x}] \quad \text{A2}$$

$$\frac{\partial f_1}{\partial x}|_{x=x_0,\Theta=\Theta_0}(x-x_0) = \{\left(\frac{1}{m_1+m_2}\right)[-0+0-k-c\frac{d}{dx}]\}(x-0) \quad \text{A3}$$

$$\frac{\partial f_1}{\partial x}|_{x=x_0,\Theta=\Theta_0}(x-x_0)=\left(\frac{1}{m_1+m_2}\right)[-kx-c\dot{x}] \quad \text{A4}$$

$$\frac{\partial f_1}{\partial \Theta}|_{x=x_0,\Theta=\Theta_0}(\Theta-\Theta_0)=\{\left(\frac{1}{m_1+m_2}\right)[-m_2R\frac{d^2}{d^2\Theta}\cos(0)-0+0+0-0-0]\}(\Theta-0) \quad \text{A5}$$

$$\frac{\partial f_1}{\partial \Theta}|_{x=x_0,\Theta=\Theta_0}(\Theta-\Theta_0)=\left(\frac{1}{m_1+m_2}\right)[-m_2R\ddot{\Theta}] \quad \text{A6}$$

$$\ddot{x}=\left(\frac{1}{m_1+m_2}\right)[-m_2R\ddot{\Theta}-kx-c\dot{x}] \quad \text{A7}$$

$$f_2(x,\Theta)=\ddot{\Theta}=\left(\frac{1}{m_2R}\right)[-(m_2\ddot{x})cos(\Theta)-m_2gsin(\Theta)-\frac{b\dot{\Theta}}{R}] \quad \text{A8}$$

$$\ddot{\Theta}=\left(\frac{1}{m_2R}\right)[-\left(m_2\frac{d^2}{dx^2}x\right)cos(\Theta)-m_2gsin(\Theta)-\frac{b\frac{d}{d\Theta}\Theta}{R}] \quad \text{A9}$$

$$\frac{\partial f_2}{\partial x}|_{x=x_0,\Theta=\Theta_0}(x-x_0)=\left(\frac{1}{m_2R}\right)\{-[\left(m_2\frac{d^2}{dx^2}\right)cos(0)-m_2gsin(0)-0]\}(x-0) \quad \text{A10}$$

$$\frac{\partial f_2}{\partial x}|_{x=x_0,\Theta=\Theta_0}(x-x_0)=\left(\frac{1}{m_2R}\right)(-m_2\ddot{x}) \quad \text{A11}$$

$$\frac{\partial f_2}{\partial \Theta}|_{x=x_0,\Theta=\Theta_0}(\Theta-\Theta_0)=\left(\frac{1}{m_2R}\right)\{-[\left(m_2\frac{d^2}{dx^2}0\right)sin(0)-m_2gcos(0)-\frac{b\frac{d}{d\Theta}}{R}]\}(\Theta-0) \quad \text{A12}$$

$$\frac{\partial f_2}{\partial \Theta}|_{x=x_0,\Theta=\Theta_0}(\Theta-\Theta_0)=\left(\frac{1}{m_2R}\right)[-m_2g(\Theta)-\frac{b\dot{\Theta}}{R}] \quad \text{A13}$$

$$\ddot{\Theta}=\left(\frac{1}{m_2R}\right)[-(m_2\ddot{x})-m_2g(\Theta)-\frac{b\dot{\Theta}}{R}] \quad \text{A14}$$

## References


[1] Celera Motion, "MicroE Optical Encoders," [Online]. Available: https://www.celeramotion.com/microe/optical-encoders/. [Accessed 3 March 2021].

[2] Omega, "Load Cells & Force Sensors," [Online]. Available: https://www.omega.com/en-us/resources/load-cells. [Accessed 3 March 2021].

[3] J. Wagner and J. Biddlecom, *ME 4440 - Mechanical Engineering Laboratory III, Laboratory Manual, Spring 2021*, pp. 1-4.